

First results of a test of a Silicon Carbide dosimeter with a neutron beam in the framework of the SAMOTHRACE project

A. Barbon,^{a,b,*} N.S. Martorana,^b G. D'Agata,^{a,b} L. Acosta,^c C. Altana,^d G. Cardella,^b A. Castoldi,^e E. De Filippo,^b S. De Luca,^d E. Geraci,^{a,b,f} B. Gnoffo,^{a,b} C. Guazzoni,^e C. Maiolino,^d E.V. Pagano,^d S. Pirrone,^b G. Politi,^{a,b} F. Risitano,^{b,g} F. Rizzo,^{a,d,f} P. Russotto,^d G. Sapienza,^d M. Trimarchi,^{b,g} S. Tudisco^d and C. Zagami^{a,d,f}

^aDipartimento di Fisica e Astronomia "Ettore Majorana",
Università degli Studi di Catania, Catania, Italy

^bINFN - Sezione di Catania, Catania, Italy

^cInstituto de Estructura de la Materia, CSIC, Spain

^dINFN - Laboratori Nazionali del Sud, Catania, Italy

^eDEIB Politecnico Milano and INFN - Sezione di Milano, Milano, Italy

^fCSFNSM, Centro Siciliano Fisica Nucleare Struttura della Materia, via S.Sofia, Catania, Italy

^gDipartimento MIFT, Università di Messina, Viale Ferdinando S. d'Alcontres, Messina, Italy

E-mail: alice_barbon@dfa.unict.it

Among the different materials used as charged particle detectors for medical and nuclear studies, Silicon Carbide has received an increasing interest from the researches thanks to its promising properties. In detail, Silicon Carbide can be used in high radiation rate environment and presents a good tissue equivalence, making it very interesting for its use as a dosimeter. In this work, the results obtained by means of tests on two different Silicon Carbide detectors with the same surface, 1 cm², and different thickness (10 μm and 100 μm) are discussed. The performances of these detectors allow to explore the possibility to use Silicon Carbide as dosimeter, micro-dosimeter and beam monitoring for radioactive ion beams, i.e. ¹¹C.

14th Young Researcher Meeting (14YRM2025)
30 September - 3 October 2025
Gran Sasso Science Institute, L'Aquila

*Speaker

1. Introduction

In recent decades, demand has grown for materials that can operate in high-radiation environments, driven by nuclear and medical physics applications. In medical physics, semiconductor radiation detectors outperform gas-filled counters by enabling faster charge collection, higher counting rates, and immediate dose response compared with passive devices such as TLDs or films. Diamond detectors have been widely investigated and show favorable dosimetric properties due to their radiation hardness and tissue-equivalent atomic number [1–3]. However, their high cost and the still-unproven superiority in absorbed-dose measurements limit their widespread adoption [4–6]. Silicon carbide (SiC) has emerged as a promising alternative, offering several advantages over silicon and diamond. In the nuclear domain, new high-intensity beam facilities—especially for radioactive ion beams [7, 8]—require robust diagnostics. The new FraISE (FRAGMENT In-flight SEPARATOR) facility under construction at LNS-INFN aims to produce RIBs with intensities of 10^3 – 10^7 pps [9–13], surpassing those previously available at FRIBs@LNS. This increase necessitates upgraded tagging and diagnostic systems. SiC devices meet these requirements and will be adopted for the new detection systems. A dedicated tagging device will be used for the CHIMERA (Charged Heavy-Ion Mass and Energy Resolving Array) multidetector beamline [14], and it will allow an event-by-event identification of the RIBs. Several physical cases will be explored within such array, such as medical applications with ^{11}C and ^{15}O [10, 15]. In the following sections, results on two different Silicon Carbide detectors will be shown: one SiC detector is conceived to be used as a beam tagging device, the other as a dosimeter and micro-dosimeter. Part of the results of SiC characterization are also reported in [16, 17, 19]. This work is part of the cooperation between the INFN-CHIRONE collaboration [20] and the SAMOTH-RACE ecosystem [22].

2. Experiment and data analysis

Two SiC devices (1 cm^2 surface, four pads each) with thicknesses of $10\text{ }\mu\text{m}$ and $100\text{ }\mu\text{m}$, respectively, were characterized.

2.1 $10\text{ }\mu\text{m}$ thick SiC

A first characterization of the $10\text{ }\mu\text{m}$ SiC, has been performed at the INFN-LNS with the use of a ^{148}Gd radioactive α -source. The aim was to study potential inter-pad effects between the four pads, cross-talk, edge effects and energy resolution. The radioactive source was placed in front of the detector, the detector was reversed bias at 40 V with an ORTEC 710 Quad 1 kV Bias Supply [21] and the system was tested under vacuum. A NeT instrument preamplifier was also operated inside the chamber. To convert and read the signals, a DT5725 CAEN digitizer (750 MHz) has been used. Figure 1 shows the SiC device on a 3D-printed support for preamplifier connection. Interpad effects were investigated using measurements with and without a collimator in front of the central pad. Figure 2 displays the energy vs rise-time scatter plots obtained without (left) and with (right) the collimator. In Figure 2 (left), the events group mainly around two areas: one with $\text{energy} > 200[\text{a.u.}]$ and $\text{rise time} < 5[\text{a.u.}]$ and another one with $150[\text{a.u.}] < \text{energy} < 200[\text{a.u.}]$ and $10[\text{a.u.}] < \text{rise time} < 20[\text{a.u.}]$. From the energy projection of these data, two peaks were highlighted. The peak at higher energy has been fitted with a Gaussian function, and a resolution of $\approx 2\%$

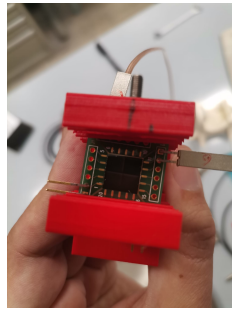


Figure 1: 10 μm thick-SiC device mounted on its support.

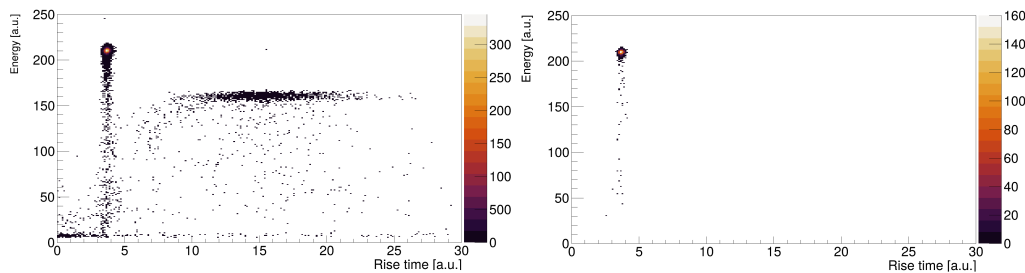


Figure 2: Plots of rise time versus energy without (left) and with (right) collimator from a 10 μm SiC .

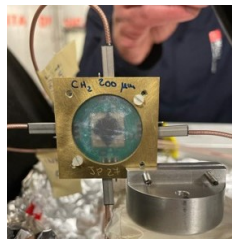


Figure 3: SiC detector 100 μm thick mounted on its support together with the CH₂ plastic.

has been obtained. It was observed that, placing a collimator in front of the SiC pad, the events corresponding to the peak in the energy plot at lower energy and higher rise-time, have been reduced (see Figure 2 right). These events have a multiplicity mainly equal to one ($\approx 90\%$), so inter-pad events or spurious cross-talk contribution are excluded. Furthermore, they can be associated with a poor charge collection on the edges of the detector [18].

2.2 100 μm thick SiC

In parallel with the previous work, a 100 μm thick SiC detector was tested. Due to its thickness, it is intended as a beam monitor, and its characterization is crucial for developing a tagging device for the CHIMERA multidetector beam line. An experimental campaign has been done at the Laboratori Nazionali di Legnaro (LNL) of INFN using a neutron beam, coming from a p+LiF reaction at 5.5 MeV. For these measurements, the SiC detector signal was processed by a Mesytec MPR-16 preamplifier. The electronic chain included a 16-channel CAEN digitizer (1 GHz) connected to a laptop for data acquisition and analysis. A 200 μm CH₂ plastic foil (Figure 3) was placed in front of the detector to induce proton production detectable by the SiC device. The

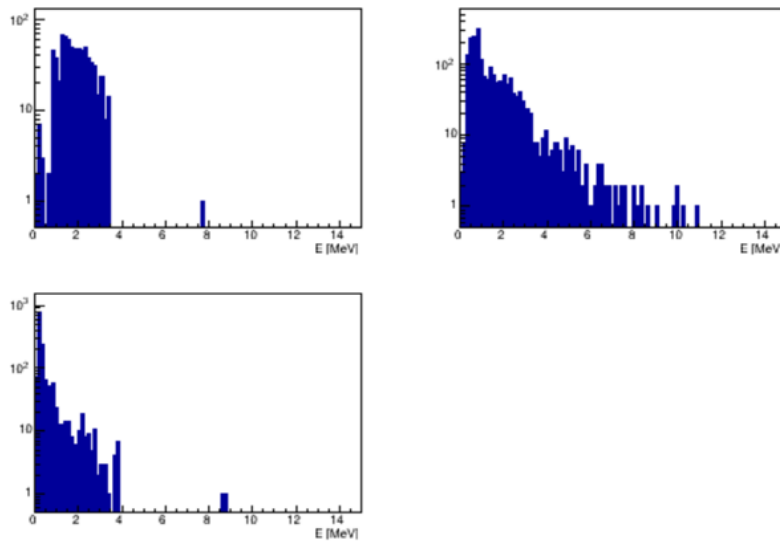


Figure 4: Calibrated experimental energy spectra of recoil protons measured in the pads of SiC detector.

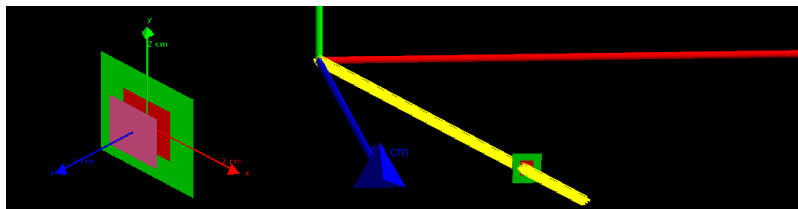


Figure 5: Left: SiC detector and CH₂ plastic reproduced in GEANT4 toolkit. Right: first simulation in GEANT4 of neutron beam impinging on the SiC device.

aim of this experiment was to test, this SiC detector under a beam and to detect charged particles. The SiC detector was reversed bias at 400 V. At the start of the experiment, pad 4 was found to be excessively noisy and was therefore disconnected and excluded from all subsequent runs. A calibration run with a mixed α source was performed a posteriori, allowing the energy range of the detected recoil protons to be determined for each remaining pad. An energy resolution around $\approx 1\%$ was obtained. The calibrated energy spectra are shown in Figure 4. Energy spectra of pads 1 and 3 end at the expected 4 MeV, while pad 2 shows some events above 4 MeV, likely due to noise; this effect is under further investigation. A GEANT4 simulation was performed to compare the expected particle production with the experimental results. First, the experimental setup geometry was simulated: a CH₂ plastic foil was placed in front of the detector, and the SiC device positioned at a precise angle to the beam line of 12° . The schematic reproduction of the SiC is shown in Figure 5 (left). The right panel shows a preliminary simulation of a neutron beam directly impinging on the SiC device. Firstly, neutrons at 4.5 MeV were simulated on the CH₂ target. The corresponding energy spectra ended around 4.5 MeV, as expected. To reproduce the experimental conditions, two neutron energies were considered (Table 1) to account for protons generated by neutrons emitted with ^7Be in both the ground and first excited states from the $^7\text{Li}(p,n)^7\text{Be}/\text{Be}^*$ reaction. The neutron beam was produced via the $p+\text{LiF}$ reaction at 5.5 MeV, yielding two neutron energies taken from

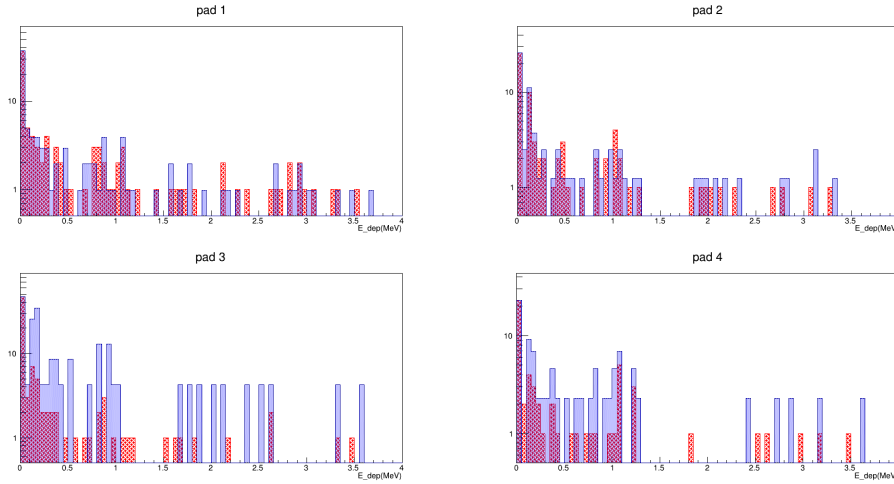


Figure 6: Simulated energy spectra of recoil protons from a neutron beam with two neutrons' energies corresponding to ${}^7\text{Li}(p,n){}^7\text{Be}$ and ${}^7\text{Li}(p,n){}^7\text{Be}^*$ reactions with energy resolution of 10% (blue) and no resolution (red).

[23]. Since the SiC detector was positioned at a specific angle and subtended a wide solid angle, an average energy corresponding to its angular acceptance was used. The contributions of the two neutron energies were then weighted according to their production branching ratios: 0.9 for the ${}^7\text{Li}(p,n){}^7\text{Be}$ reaction and 0.1 for the ${}^7\text{Li}(p,n){}^7\text{Be}^*$ reaction. To enable a rigorous comparison with

Table 1: Neutrons' energy from Liskien and Paulsen's article [23].

Reaction	θ [deg]	E [MeV]
${}^7\text{Li}(p,n){}^7\text{Be}^*$	10	3.368
${}^7\text{Li}(p,n){}^7\text{Be}^*$	15	3.344
${}^7\text{Li}(p,n){}^7\text{Be}$	10	3.814
${}^7\text{Li}(p,n){}^7\text{Be}$	15	3.789

the experimental data, the detector resolution of 10 % was included in the GEANT4 simulation. This value was adopted as an initial assumption and will be examined in greater detail in future studies. Figure 6 shows the simulated energy spectra (red) for the four pads, all terminating around 3.5 MeV and displaying good preliminary mutual consistency. To reproduce the detector response, the GEANT4 simulation was extended to include the SiC energy resolution by introducing a 10% energy spread for the recoil protons. The two neutron energies, weighted by their branching ratios, were again considered. Figure 6 compares the spectra without resolution (red) and with a 10% resolution (blue), showing a broadening when the resolution is included. Further refinements will be implemented to better match the experimental data.

3. Results and conclusions

Two SiC devices were analyzed. The first, a 10 μm -thick device intended for dosimetry and micro-dosimetry, was characterized using a ${}^{148}\text{Gd}$ α source to investigate possible inter-pad, cross-talk and edge effects. The second, a 100 μm -thick device, designed as a beam monitor, was tested with neutrons incident on a CH_2 target. Experimental results were compared with GEANT4 simulations. Future work on the 10 μm device will focus on dose extraction and comparison with other

detectors, while studies on the 100 μm device will refine GEANT4 and SYNOPSIS simulations, particularly regarding the energy resolution. This work has been partially funded by the European Union-(NextGeneration EU), through MURPNRR project SAMOTHRACE (ECS00000022).

References

- [1] B. Plansky, *Physics in Medicine and Biology* 25:3 (1980).
- [2] M. Heydariyan et al., *Physics in Medicine and Biology* 38:8 (1993).
- [3] S. Vatsnitsky and H. Jarvinen, *Physics in Medicine and Biology* 38:1 (1993).
- [4] S. Onori et al., *Physics in Medicine and Biology* 45:10 (2000).
- [5] A. Fidanzio et al., *Medical Physics* 29:5 (2002).
- [6] U. Sowa et al., *Nukleonika* 57:4 (2012).
- [7] M. Ballan et al., *European Physical Journal Plus* 138:709 (2023).
- [8] C. Agodi et al., *European Physical Journal Plus* 138:1038 (2023).
- [9] N.S. Martorana, *Il Nuovo Cimento* 44(C):1 (2021).
- [10] N.S. Martorana et al., *Frontiers in Physics* 10 (2022).
- [11] P. Russotto et al 2018 *J. Phys.: Conf. Ser.* 1014 012016.
- [12] N.S. Martorana et al., *Il Nuovo Cimento* 45(C):63 (2022).
- [13] N.S. Martorana et al., *Journal of Physics: Conference Series* 2586:012149 (2023).
- [14] CHIMERA detector, <https://web.infn.it/CHIMERA/index.php/en/detectors>
- [15] M. Durante and K. Parodi, *Frontiers in Physics* 8:326 (2020).
- [16] G. D'Agata et al., *Il Nuovo Cimento* 48(C):72 (2025).
- [17] N.S. Martorana et al., *Il Nuovo Cimento* 48(C):62 (2025).
- [18] N. S. Martorana et al., *Nuclear Inst. and Methods in Physics Research, A* 1086 (2026) 171356.
- [19] A. Barbon et al., *Il Nuovo Cimento* 48(C):70 (2025).
- [20] CHIRONE collaboration, <https://web.infn.it/CHIMERA/index.php/it/collaborazione-chirone>
- [21] Ortec Quad Bias Supply, <https://www.ortec-online.com/products/electronic-instruments/nim-power-supplies-and-bins/710>
- [22] SAMOTHRACE project, <https://samothrace.eu>
- [23] H. Liskien and A. Paulsen, *Atomic Data and Nuclear Data Tables* 15 (1975).